Nuclear Engineering and Technology 54 (2022) 3398–3402

Contents lists available at ScienceDirect

Nuclear Engineering and Technology

journal homepage: www.elsevier.com/locate/net

Original Article

# Measurements of low dose rates of gamma-rays using position-sensitive plastic scintillation optical fiber detector

Siwon Song, Jinhong Kim, Jae Hyung Park, Seunghyeon Kim, Taeseob Lim, Jin Ho Kim, Sin Kim, Bongsoo Lee*

*School of Energy Systems Engineering, Chung-Ang University, Seoul, 06974, South Korea*

ARTICLE INFO

*Article history:*
Received 8 February 2022
Received in revised form
16 March 2022
Accepted 30 March 2022
Available online 2 April 2022

*Keywords:*
Gamma-ray source position
Plastic scintillation optical fiber
Radiation monitoring
Low dose rate gamma-ray
Gamma-ray dose rate measurement

ABSTRACT

We fabricated a 15 m long position-sensitive plastic scintillation optical fiber (PSOF) detector consisting of a PSOF, two photomultiplier tubes, four fast amplifiers, and a digitizer. A single PSOF was used as a sensing part to estimate the gamma-ray source position, and $^{137}$Cs, an uncollimated solid-disk-type radioactive isotope, was used as a gamma-ray emitter. To improve the sensitivity, accuracy, and measurement time of a PSOF detector compared to those of previous studies, the performance of the amplifier was optimized, and the digital signal processing (DSP) was newly designed in this study. Moreover, we could measure very low dose rates of gamma-rays with high sensitivity and accuracy in a very short time using our proposed PSOF detector. The results of this study indicate that it is possible to accurately and quickly locate the position of a very low dose rate gamma-ray source in a wide range of contaminated areas using the proposed position-sensitive PSOF detector.
© 2022 Korean Nuclear Society, Published by Elsevier Korea LLC. This is an open access article under the CC BY-NC-ND license (http://creativecommons.org/licenses/by-nc-nd/4.0/).

## 1. Introduction

After the Fukushima Daiichi Nuclear Power Plant (FDNPP) accident (2011), large quantities of radionuclides were released into the environment [1]. The most significant long-lived artificial radionuclides released from such accidents were $^{137}$Cs and $^{134}$Cs, with a total emission of about 20 PBq [2]. In particular, $^{137}$Cs has a long-term radiation problem because of its long half-life and strong adsorption to soil particles [3]. To understand the stabilization and decontamination phenomena of radionuclides in large-scale nuclear accidents, it is essential to identify radiation hotspots. Monitoring of dispersed radionuclides during and after decontamination is also necessary to evaluate the decontamination process [4].

There exist mainly three methods for performing radiation monitoring in contaminated areas. Such methods are divided into static ground-based, mobile ground-based, and airborne surveys [5]. The static ground-based survey is limited to the location of ground stations; however, the data are limited to the vicinity of these stations [6]. Surveying of contaminated areas for large-scale radiation events, on the other hand, is possible using airborne or mobile ground-based surveys. Mobile ground-based surveys provide superior spatial resolution compared to aerial surveys but require significant data collection time over larger areas. Therefore, the sensitivity and measurement time are essential for the detectors used in mobile-based surveys to find the hotspots with accuracy in a short period of time.

A plastic scintillation optical fiber (PSOF) detector can be used to localize and quantify radiation sources in a wide range of contaminated areas. The long position-sensitive detectors, using a PSOF, are generally easy to configure and reliable for finding the position of radioisotopes based on a simple principle [7]. A PSOF has many advantages such as good flexibility, long length usability, cost-effectiveness in manufacturing, high water resistance, and lack of interference from electromagnetic fields [8].

Normally, the PSOF detector provides one-dimensional data on the contaminated area, enabling faster measurements than conventional point-measuring static ground-based detectors. It can also be used for two-dimensional area surveys by moving in the perpendicular direction. After the FDNPP accident, the Japan Atomic Energy Agency (JAEA) operated a PSOF detector for on-site surface contamination surveys in forested areas and measured radioactive cesium concentrations at the bottom of an irrigation pond in Fukushima [9,10]. In addition, the monitoring data measured by the PSOF detectors were used to evaluate the ecological half-life of radioactive cesium concentrations in

* Corresponding author.
*E-mail address:* bslee@cau.ac.kr (B. Lee).

https://doi.org/10.1016/j.net.2022.03.043
1738-5733/© 2022 Korean Nuclear Society, Published by Elsevier Korea LLC. This is an open access article under the CC BY-NC-ND license (http://creativecommons.org/licenses/by-nc-nd/4.0/).

sediments of five ponds in Fukushima from 2013 to 2019 [11].

As gamma-rays interact with the PSOF, scintillation light is emitted in the 4π direction, which is transmitted to both ends of the PSOF through total internal reflection. The time-of-flight (TOF) method was mainly used in previous studies to estimate the position of the gamma-ray source using the PSOF detector. Soramoto et al. [12], Emoto et al. [13], Nohtomi et al. [7], Chichester et al. [14], Gamo et al. [15], and Song et al. [16] estimated the position of the gamma-ray source using the TOF method. They measured a difference in the time of the scintillation light signal according to the difference in the transmission path of the scintillation light reaching both ends of the PSOF and estimated the position of the gamma-ray source.

The dose rate of the gamma-ray also can be determined through the counting rate for the position of the source in the PSOF detector; however, few studies that investigate dose rates have been reported till now [13–15]. Especially, to measure low dose rates of radioisotope properly with a PSOF detector, the sensitivity is very important, and the count rates of the detector should be enough. Emoto et al. firstly could measure the dose rate of gamma-ray using a PSOF, however the count rates were too low and the measurement time was too long [13]. Chichester et al. and Gamo et al., also measured the dose rates of $^{137}$Cs gamma sources using a PSOF with limited minimum dose rates such as 12 and 0.1 μSv/h, respectively [14,15].

In this study, a position-sensitive PSOF detector was developed using a single strand of PSOF with a length of 15 m and a diameter of 2 mm. To improve the sensitivity and accuracy of the PSOF detector, the performance of the amplifier was optimized, and the digital signal processing (DSP), which removes the high and low frequency noises of the signals, was newly designed. In addition, the unwanted signals caused by the dark currents of the photomultiplier tube (PMT) were removed using a DSP to measure very low dose rates of gamma-rays. The proposed PSOF detector could measure the dose rates of $^{137}$Cs gamma sources in the range of 0.045–12 μSv/h for 60 s, which are much lower dose rates and faster measurement time compared to the results of the previous studies.

## 2. Materials and methods

The position-sensitive PSOF detector in this study consisted of a PSOF, two PMTs (H6533, Hamamatsu Photonics), four fast amplifiers (ABL0300-00-4030, WENTEQ & A1424, CAEN), and a digitizer (DT5742, CAEN). The sensing part is made up of a PSOF (SCSF-78, Kuraray) of diameter 2.0 mm and length 15 m. The selected PSOF emitted blue light with a peak wavelength of 450 nm and has a multi-cladded structure. The trapping efficiency of a multi-cladded PSOF is about 5.4%, which is higher than that of a single-cladded PSOF. Both the inner and outer cladding thicknesses are 0.04 mm, that is, 2% of the PSOF diameter [17]. The materials of the core, the inner and outer cladding are polystyrene (PS), polymethyl methacrylate (PMMA), and fluorinated polymer (FP), respectively. The refractive indices of the PS, PMMA, and FP are 1.59, 1.49, and 1.42, respectively, and the numerical aperture (NA) is 0.72. The NA denotes the light-gathering power, implying more light can be guided by a PSOF with a higher NA [18]. The decay time and attenuation length of the PSOF are 2.8 ns and 4 m, respectively.

The emitting gamma-rays from $^{137}$Cs (Epeak = 661.66 keV) interact with PS in the core material, and its average atomic number is about 5.6, and causing Compton scatterings are in most cases [19,20]. The Compton edge energy of $^{137}$Cs is 447.34 keV, and the recoiled electron of that energy has a continuous slowing-down approximation (CSDA) of about 1.6 mm in PS [21]. Considering the CSDA of the PSOF, the diameter of the PSOF is selected as 2 mm.

A PSOF was packed within a light-tight, flexible black shrink tube (FP-301, 3 M). Both ends of the PSOF were polished with various sizes and types of polishing pads. The PSOF was optically coupled with silicone-rubber-based optical interfaces (EJ-560, Eljen Technology) to the windows of the PMTs. Fig. 1 presents a photograph of the end setup of the polished PSOF and an assembly after combining the PSOF and the PMTs. Fig. 2 shows the overall experimental setup. The $^{137}$Cs uncollimated source was placed close under the PSOF, and the scintillation light generated from the PSOF was transmitted to two PMTs, which were placed at both ends of the PSOF as light-measuring devices. The PMT has a maximum sensitivity at a wavelength of 420 nm. The output current signals of the PMTs were amplified using fast amplifiers and sampled using a digitizer. Two fast amplifiers are connected in series per one PMT to improve the sensitivity of the PSOF detector and the amplification ratios of them were optimized for the dynamic range of the digitizer. A digitizer with a sampling rate of 5 GS/s was used to obtain signal data close to the original ones generated from the PMTs.

Fig. 3 shows the flow chart of the DSP designed using Matrix Laboratory (MATLAB) to estimate exact positions and dose rates of gamma-emitting radionuclides. High and low frequency noises in the signals acquired from the digitizer are removed through the wavelet signal denoising (WSD) method. Wavelet is a mathematical tool that divides the original signal into different frequency components and examines each component individually. It removes noises from the signals through the process of decomposition, detail coefficients thresholding, and reconstruction [22]. Moreover, cubic spline interpolation (CSI) was applied to the signal data acquired by the digitizer. The values at query points were based on the CSI of the values of neighboring data points. The signal data acquired from the digitizer were made comparable to the original signal using the WSD method and the CSI to improve the accuracy of the data [23,24].

The position of the $^{137}$Cs gamma-ray source was estimated through constant fraction triggering (CFT). Generally, leading-edge triggering using a constant threshold value causes timing errors



**Fig. 1.** Photograph of the end of the polished PSOF and an assembly after combining the 15 m length PSOF and two PMTs.

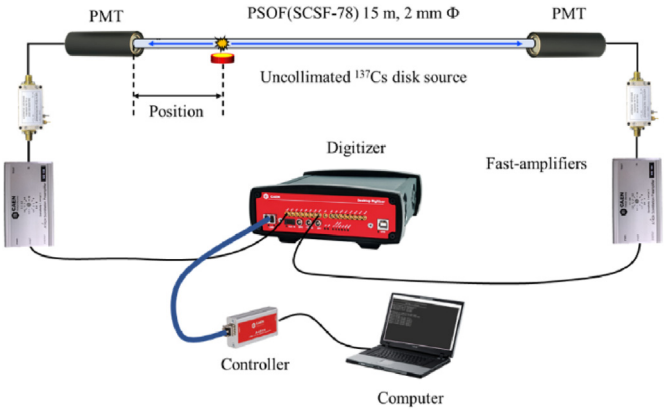



**Fig. 2.** Illustration of the experimental setup for measuring the position and dose rates of a $^{137}$Cs gamma-ray source using the position-sensitive PSOF detector.

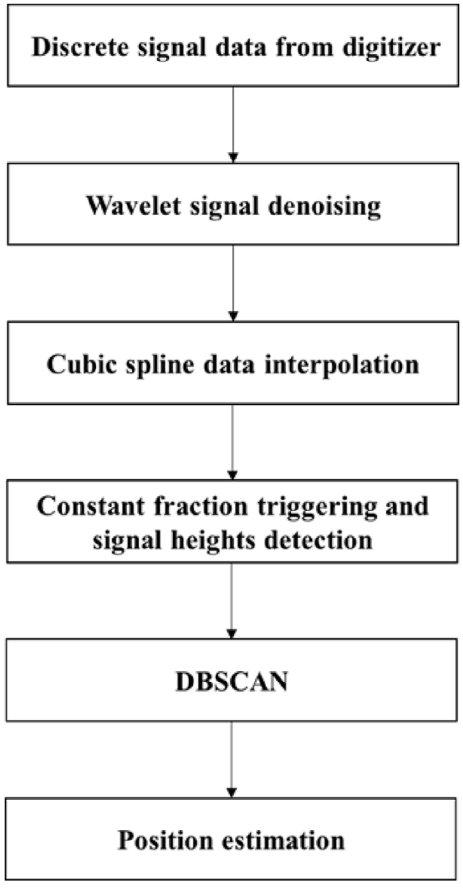



**Fig. 3.** Flow chart of the DSP designed using MATLAB.

due to the walk effect. Even coincident signals of differing heights exhibit a walk effect. In the case of CFT, the threshold value is proportional to the height of the signal and walk-free triggering is possible when the rise time of the signals is constant [25].

To remove unwanted signals caused by the dark currents of the PMTs from the measured position spectrum, a scatter plot composed of the time and height differences of the signals from both PMTs is drawn. Density-based spatial clustering of applications with noise (DBSCAN) was applied to the scatter plot to remove the unwanted signals in the measured position spectrum. DBSCAN is a clustering algorithm based on data point distribution density, which can identify the degree of data and classify the data points in the distribution. Normally, it can be used to distinguish between clusters and noises in data in many fields [26].

Fig. 4 shows the position spectra according to DSP applications. By increasing the triggering accuracy through WSD and CSI, the peak of position spectrum increases and the full width at half maximum (FWHM) decreases. Additionally, it is possible to remove noises with same peak height of position spectrum using DBSCAN and the final position spectrum with Gaussian fitting can be obtained.

## 3. Experimental results

A position-sensitive PSOF detector must measure enough counts for Gaussian fitting to estimate spatial resolution of the gamma-ray source position in the measurement time. Normally, the spatial resolution of the position-sensitive PSOF detector can be denoted by FWHM of a Gaussian curve fitted at the measured position spectrum. Fig. 5 shows the measured position spectra of a $^{137}$Cs gamma-ray source (0.22 μCi) placed at the center of the PSOF according to measurement time. As measurement time increases, the number of counts also increases although the FWHMs of the Gaussian curves do not change much. As shown in Fig. 6, the average value of FWHMs is 0.47 m, and their deviations are in the range of 0.436–0.493 m for the measurement times of 10–60 s; however, the standard deviation of the FWHMs at the measurement time are reduced as measurement time increases. The average FWHM and its standard deviation measured for 60 s are 0.480 ± 0.024 m, showing higher spatial resolution of the position-sensitive PSOF detector compared to that of the previous study [14].

Fig. 7 also shows the variations in estimated positions of a $^{137}$Cs gamma-ray source according to measurement time. The source position is estimated by the peak value of a fitted Gaussian curve, and this value normally varies with measurement time. As shown in Fig. 6, the measured variations of FWHMs and average values are obtained through repeated experiments and the average value and standard deviation of the position for 60 s is 7.522 ± 0.007 m, which is the smallest.

The count rate of the PSOF detector is integral to measure the dose rates of a gamma-ray source, which must be stable and high enough to obtain a reliable dose rate. The average count rate and its standard deviation is 7.68 ± 0.3 counts/s for 60 s, which can be converted into 170.58 ± 6.67 counts/s per μSv/h. According to the results as shown in Figs. 6 and 7, the optimized measurement time can be determined as 60 s with smallest standard deviations of measured FWHMs and estimated positions at every measurement time.

Fig. 8 shows the linear relationship between the total count and measurement time of the PSOF detector. It is found that the average count increases linearly with increasing measurement time with an accuracy of about 99.7%.

The annual exposure dose limit for the general public set by the ICRP is 1 mSv, which can be converted into a dose rate of about 0.11 μSv/h [27]. The Republic of Korea operates an integrated environmental radiation monitoring network (IERNet) to monitor radiological emergencies that may affect the country due to domestic and overseas nuclear accidents. IERNet is divided into four levels: normal, attention, warning, and emergency; levels are set to less than 0.0973 μSv/h, 0.0973 μSv/h or more, 0.973 μSv/h or more, and 973 μSv/h or more, respectively, based on the average dose rate of the corresponding point.

In this study, the count rates of the PSOF detector were evaluated for a low dose rate of $^{137}$Cs gamma-ray source from 0.045 to

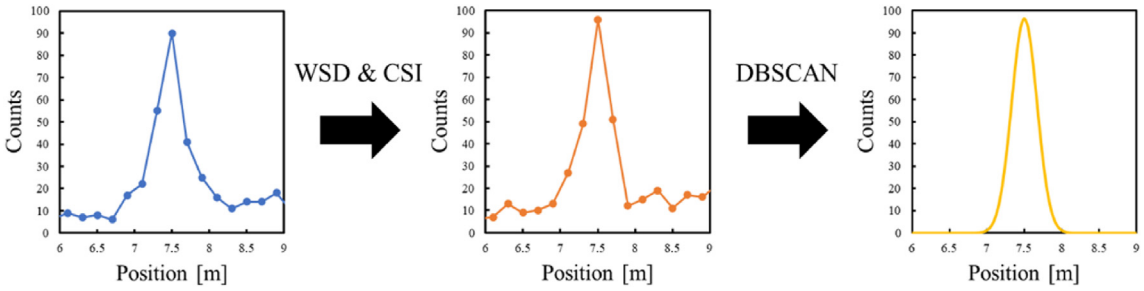



**Fig. 4.** Position spectra according to DSP.

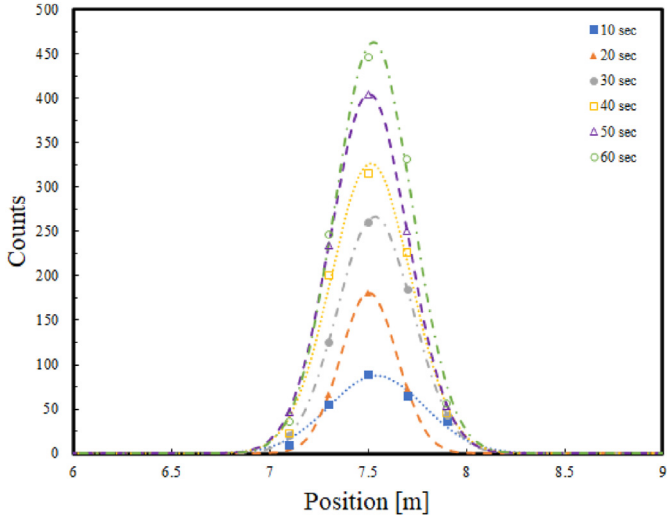



**Fig. 5.** Measured position spectra and fitted Gaussian curves for determining measurement times.

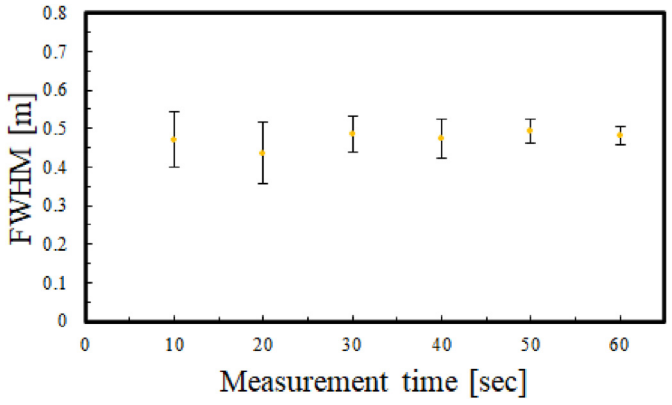



**Fig. 6.** The variations of the FWHM according to measurement time.

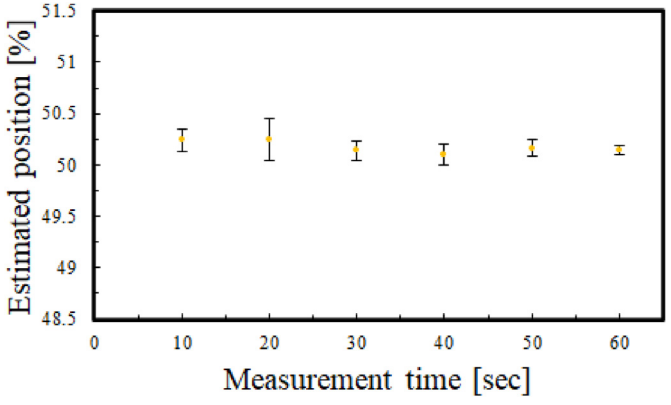



**Fig. 7.** The variations of the estimated positions according to measurement time.

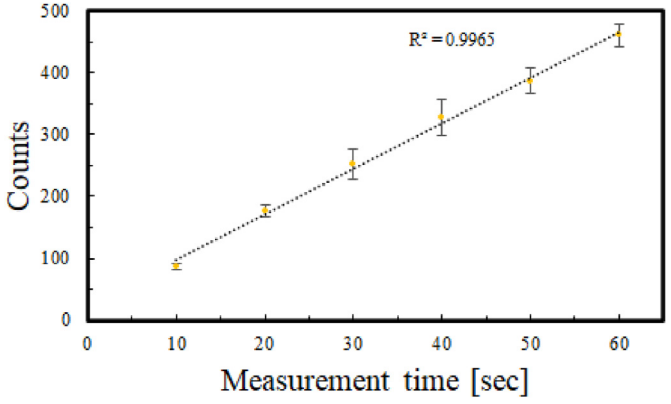



**Fig. 8.** Linearity of counts over measurement time.

12.022 μSv/h. Fig. 9 shows measured count rates using the proposed PSOF detector according to the dose rates when the $^{137}$Cs gamma-ray sources with different activities (0.22, 0.38, 3.75 and 7.5 μCi) are positioned at 5 m for 60 s and such values are consistent with a calibrated survey meter (451B, Fluke). Currently, few studies that measure gamma-ray dose rates using a position-sensitive PSOF detector have been reported. The INL reported that they fabricated a position-sensitive PSOF bundle detector comprising ten PSOFs whose diameter and length are 1 mm and 15 m, respectively. As shown in Fig. 9, they measured the dose rates of a $^{137}$Cs gamma-ray source within the range of 12–140 μSv/h with the same 15 m PSOF detector as used in this study. Their measurement time was reported as 900 s to estimate each dose rate and the INL could not measure a minimum dose rate below 12 μSv/h due to low sensitivity and long measurement time of their PSOF detector. Another study was done by Hitachi-GE Nuclear Energy, and they also reported that the dose rates of a $^{137}$Cs gamma-ray source were measured in the range of 0.1–8 μSv/h with a high-sensitive PSOF bundle detector. Even they measured lower dose rates compared to that of INL, they also used twelve PSOFs to increase the sensitivity of their position-sensitive detector [15]. However, we could measure the minimum dose rate of 0.045 μSv/h with $^{137}$Cs gamma-ray source for 60 s, which is less than the minimum level in the IER-Net classification. As shown in Fig. 9, the count rate of the proposed

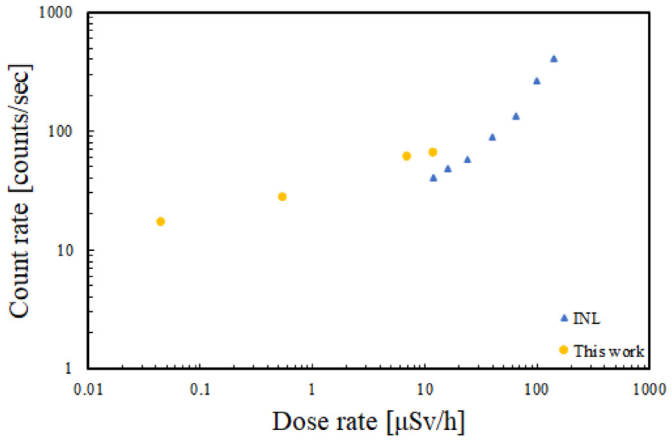



**Fig. 9.** The variation of count rates according to the dose rate of $^{137}$Cs gamma-ray source.

PSOF detector is higher than that of the INL at the same dose rate of 12 μSv/h, indicating that our detector is more sensitive by about 1.60 times.

## 4. Conclusion

In this study, a position-sensitive PSOF detector was constructed, and its performance was evaluated. The proposed PSOF detector consists of a multi-coated PSOF, two PMTs, four high-speed amplifiers, and a digitizer. To improve the sensitivity and accuracy of the proposed PSOF detector, two fast amplifiers were connected series for both PMTs and the amplification ratio was optimized. In addition, the newly designed DSP removed high and low frequency noises from the signals and the unwanted signals caused by the dark current of the PMT were also removed using a DBSCAN to accurately measure the dose rate. We noticed that the improved sensitivity and accuracy allowed the PSOF detector to measure very low dose rates of gamma-ray much faster. The sensitivity of our proposed PSOF detector was significantly improved over other PSOF detectors, and the measured minimum dose rate for $^{137}$Cs gamma-ray source was 0.045 μSv/h. The efficiency of the proposed PSOF detector is about 170.59 counts/s per μSv/h, which is a much higher value than the value, 2.69 counts/s per μSv/h, reported in a previous study for a 15 m long PSOF bundle detector [14]. In addition, the volume of the PSOF used to fabricate the detector can be reduced to 33–57% of the existed PSOF bundle detectors reported and the measurement time is also reduced to 60 s to measure very low dose rates of $^{137}$Cs gamma-rays, which is much shorter time compared to that reported in a previous study [14,15]. The PSOF detector proposed in this study can be used to locate gamma-ray emitting radioisotopes quickly and to measure very low dose rates of gamma-rays accurately. In future studies, a two-dimensional PSOF detector will be fabricated to find the positions and measure dose rates of gamma-ray emitting radionuclides over a larger contaminated area in shorter time.

## Declaration of competing interest

The authors declare that they have no known competing financial interests or personal relationships that could have appeared to influence the work reported in this paper.

## Acknowledgements

This work was supported by the Chung-Ang University Research Scholarship Grants in 2019 and a National Research Foundation of Korea (NRF) grant funded by the Korean government (MSIT) (No. 2020M2D2A2062457, No. 2020M2D8A2066404).

## References

[1] S. Endo, S. Kimura, T. Takatsuji, K. Nanasawa, T. Imanaka, K. Shizuma, Measurement of soil contamination by radionuclides due to the Fukushima Daiichi Nuclear Power Plant accident and associated estimated cumulative external dose estimation, J. Environ. Radioact. 111 (2012) 18–27.
[2] H. Terada, H. Nagai, K. Tsuduki, A. Furuno, M. Kadowaki, T. Kakefuda, Refinement of source term and atmospheric dispersion simulations of radionuclides during the Fukushima Daiichi Nuclear Power Station accident, J. Environ. Radioact. 213 (2020), 106104.
[3] H. Mukai, A. Hirose, S. Motai, R. Kikuchi, K. Tanoi, T.M. Nakanishi, T. Yaita, T. Kogure, Cesium adsorption/desorption behavior of clay minerals considering actual contamination conditions in Fukushima, Sci. Rep. 6 (2016), 21543.
[4] S.D. Lee, Current and Emerging Post-Fukushima Technologies, and Techniques, and Practices for Wide Area Radiological Survey, Remediation, and Waste Management, EPA, 2016, p. 11. EPA/600/R-16/140.
[5] D. Connor, P.G. Martin, T.B. Scott, Airborne radiation mapping: overview and application of current and future aerial systems, Int. J. Rem. Sens. 37 (2016) 5953–5987.
[6] A.A. Green, Leveling airborne gamma-radiation data using between-channel correlation information, Geophysics 52 (1987) 1557–1562.
[7] A. Nohtomi, N. Sugiura, T. Itho, T. Torii, On-line evaluation of spatial dose-distribution by using a 15m-long plastic scintillation-fiber detector, in: Proceedings of 2008 IEEE Nuclear Science Symposium Conference Record, 2008, pp. 19–25 (October, Dresden, Germany).
[8] S.D. Lee, Plastic Scintillation Fibers for Radiological Contamination Surveys, EPA, 2018, pp. 2–3. EPA/600/R-17/370.
[9] J. Koarashi, M. Atarashi-Andoh, T. Matsunaga, Y. Sanada, Forest type effects on the retention of radiocesium in organic layers of forest ecosystems affected by the Fukushima nuclear accident, Sci. Rep. 6 (2016) 38591.
[10] C. Masamichi, JAEA R&D Review 2014, JAEA, 2015, p. 14.
[11] E.W. Katengeza, Y. Sanada, K. Yoshimura, K. Ochi, T. Iimoto, The ecological half-life of radiocesium in surficial bottom sediments of five ponds in Fukushima based on in situ measurements with plastic scintillation fibers, Environ. Sci. Process. 22 (2020) 1566–1574.
[12] S. Soramoto, M. Notani, Y. Fukano, S. Imai, T. Iguchi, M. Zakazawa, A study of distributed radiation sensing method using plastic scintillation fiber, in: Proceedings of the 7th Workshop on Radiation Detectors and Their Uses, 1993, pp. 26–27. January, Tsukuba, Japan.
[13] T. Emoto, T. Trorii, T. Nozaki, H. Ando, Measurement of spatial dose-rate distribution using a position sensitive detector, in: Proceedings of the 8th Workshop on Radiation Detectors and Their Uses, 1994, pp. 25–27. January, Tsukuba, Japan.
[14] D.L. Chichester, S.M. Watson, J.T. Johnson, Comparison of BCF-10, BCF-12, and BCF-20 scintillation fiber use in a 1-dimensional linear sensor, in: Proceedings of the IEEE Nuclear Science Symposium and Medical Imaging Conference Record, 2012, 29 October-3 November, CA, USA.
[15] H. Gamo, M. Kondo, T. Hashimoto, R. Yayama, T. Tsukiyama, Development of a PSF-detector for contaminated areas, Prog. Nucl. Energy 4 (2014) 695–696.
[16] S. Song, J. Kim, J.H. Park, S. Kim, T. Lim, J.H. Kim, J.H. Moon, B. Lee, High-spatial-resolution position-sensitive plastic scintillation optical fiber bundle detector, Photonics 8 (2021) 26.
[17] Kuraray, Plastic scintillating fibers, Available online: https://www.kuraray.com/uploads/5a717515df6f5/PR0150_psf01.pdf.
[18] K.W. Jang, W.J. Yoo, J. Moon, K.T. Han, J.-Y. Park, B. Lee, Measurements of relative depth doses and cerenkov light using a scintillating fiber-optic dosimeter with Co-60 radiotherapy, Appl. Radiat. Isot. 70 (2012) 275.
[19] R.L. Heath, Scintillation Spectrometry gamma-ray spectrum Catalogue, Available online: https://gammaray.inl.gov/Shared%20Documents/naicat.pdf..
[20] NIST, XCOM Photon Cross Sections Database, Available online: http://physics.nist.gov/PhysRefData/Xcom/html/xcom1.html.
[21] NIST, Standard Reference Database 124, Available online: https://physics.nist.gov/cgi-bin/Star/e_table.pl.
[22] Ç.P. Dautov, M.S. Özerdem, Wavelet transform and signal denoising using Wavelet method, in: Proceedings of 2018 26th Signal Processing and Communications Applications Conference, 2018, pp. 2–5. May, Izmir, Turkey.
[23] R.J. Aliaga, Real-time estimation of zero crossings of sampled signals for timing using cubic spline interpolation, IEEE Trans. Nucl. Sci. 64 (2017) 2414–2422.
[24] MathWorks, MATLAB Function Reference, Available online: https://kr.mathworks.com/help/pdf_doc/matlab/matlab_ref.pdf.
[25] W.R. Leo, Techniques for Nuclear and Particle Physics Experiments, second ed., Springer, New York, 1994.
[26] M. Ester, H.-P. Kriegel, J. Sander, X. Xu, Proceedings of the Second International Conference on Knowledge Discovery and Data Mining, 1996, pp. 2–4. August, OR, USA.
[27] ICRP, The 2007 recommendations of the international commission on radiological protection, ICRP Publ. 103 Ann ICRP. 37 (2007) 36–131.